

See discussions, stats, and author profiles for this publication at: <https://www.researchgate.net/publication/228935188>

On the synthesis of guitar plucks

Article in *Acta Acustica united with Acustica* · September 2004

CITATIONS

84

READS

1,130

1 author:



[Jim Woodhouse](#)

University of Cambridge

230 PUBLICATIONS 7,027 CITATIONS

SEE PROFILE

On the Synthesis of Guitar Plucks

J. Woodhouse

Cambridge University Engineering Department, Trumpington St, Cambridge CB2 1PZ, UK.

jw12@eng.cam.ac.uk

Summary

Several different approaches are described to the problem of synthesising the pluck response of a guitar, starting from information about string properties and the input admittance at the bridge of the guitar. Synthesis can be carried out in the frequency domain, the time domain, or via modal superposition. Within these categories there are further options. A range of methods is developed and implemented, and their performance on a particular test case compared. The two most successful methods are found to be modal synthesis using the first-order method, and frequency-domain synthesis. Of the two, frequency domain synthesis proves to be faster. A significant conclusion is that the coupled string/body modes of a normal classical guitar do not show “veering” behaviour except at low frequencies, so that it is important to use a synthesis method which incorporates fully the effect of string damping: methods based on first finding undamped modes give poor results.

PACS no. 43.40.Cw, 43.75.Gh

1. Introduction

On the face of it, vibrational analysis of the guitar is rather simple. When a guitar string is plucked the player creates certain initial conditions of displacement and velocity in the string and the guitar body, then releases the string so that they vibrate freely. Provided the motion is small enough for linear theory to apply, the resulting vibration and sound radiation is given simply by a superposition of the transient responses of the various coupled string/body modes of the instrument. (“Body” is used here to include the effect of the air within the cavity and outside.) The player can, to a certain extent, control the amplitudes making up the modal mixture, but the frequency, decay rate and radiation behaviour of each mode are governed by the instrument’s construction and stringing, and the player can only exert a very minor influence on them for musical effect.

Somewhere in the details of these transient decaying sounds lies the information which determines perceptual judgements: discrimination and quality rating between instruments, and the musical “palette” available to the player. It is not clear precisely which features of these transients have audible consequences: it is likely that in the context of musical performance, rather subtle effects may sometimes matter. In pursuit of the goal of relating musical qualities to the constructional details of an instrument it is necessary to develop theoretical models of the system, and to be useful such models must be capable of achieving an accurate match to the observed physical behaviour of an instrument. In this paper, various possible approaches

to the synthesis of plucked-string transients are examined, and in a companion paper [1] the predictions are compared with measurements.

The vibration of an ideal stretched string is treated in every vibration textbook, and the specific behaviour of musical strings has also been researched extensively (see for example [2, 3, 4]). Similarly, many measurements have been published of the vibration behaviour of guitar and violin bodies (see for example [2, 5]). It seems remarkable, therefore, that there is no published work which explores all the issues of putting the two together to give a fully detailed method to synthesise the coupled string/body vibration from the separate knowledge of string and body behaviour. Parts of the problem have been tackled, certainly. A thorough and insightful treatment has been given by Gough [6] of the coupling of one string overtone to one mode of an instrument body. The specific coupled vibration problem of the cello’s wolf note has been discussed by several authors (e.g. Schelleng [7]). In a very recent study, Derveaux *et al.* [8] have presented numerical simulations which include a string, an idealised guitar body and the surrounding air. There is also an extensive literature on the general problem of computational methods for vibration analysis of complex structures, including methods based on assembling the behaviour of a complete system from results for separate subsystems (see for example [9]).

However, none of these treatments entirely addresses the problem of synthesis of the transient response to a pluck over the full frequency range of interest for musical applications. That is the task of this paper, and the attempt to solve it and to compare the results with measurements will reveal some surprising subtleties. Many of these are associated in one way or another with the correct treatment of vibration damping: after all, one of the major

Received 1 October 2003,
accepted 26 March 2004.

criteria for a successful synthesis method is that it should give good predictions of decay rates. These vary strongly with frequency, and reproducing this pattern by synthesis is a challenging problem.

It should be emphasised that the objective here is to develop synthesis methods which are physically accurate in the sense of matching in as much detail as possible the measured behaviour of real guitars. The purpose of the models is primarily to address questions of interest to acoustical guitar makers and players, so that it is important to keep a clear link between physical parameters of the instrument and the parameters of the model. This results in significantly different priorities to work which is concerned with designing synthesis algorithms for real-time musical performance (see for example [10]). The emphasis there is inevitably on making such simplifications as are possible without sacrificing too much in sound quality, in the interests of speed. The approach taken here is to defer questions about auditory consequences until the model has been demonstrated “complete” by laboratory measurements. It will then be possible to proceed by subtraction, suppressing details of the model and assessing by listening tests whether the change is significant to a listener or player of the guitar.

It is worth noting the complexity of the synthesis task. The radiated sound from a typical note on a classical guitar shows clear spectral peaks up to at least 5 kHz. This gives a useful target frequency range for synthesis. It corresponds to about the 60th harmonic of the lowest note on a normal guitar (82 Hz). Each of these isolated string “harmonics” can appear in two polarisations. A typical guitar body structure has of the order of 250 vibration modes in this range (plus a roughly comparable number of modes of the internal air cavity [11]). Assembling these numbers, it is clear that an accurate synthesis method may have to account correctly for several hundred degrees of freedom. It may come as a surprise to learn that very few vibration predictions of this degree of complexity have ever been confirmed in detail by experiment. Although very large Finite-Element models are routinely used for vibration prediction of industrial structures of many kinds, where these have been checked against measurements they rarely give full agreement in detail beyond the first few modes (although qualitative and statistical aspects of the predictions may work to higher frequencies). Not for the first time, musical acoustics is “pushing the envelope” of vibration analysis.

2. Overview of synthesis methods

2.1. Characterising string and body

There is a wide variety of possible approaches to synthesis. Before going into details, it is useful to review these methods in outline and note their potential strengths and weaknesses. All methods start from the same basic information. The string is characterised by a small number of fundamental physical properties: tension, mass per unit length, bending stiffness and damping. Other relevant properties, such as wave speed and characteristic impedance, follow from these. Symbolically, the string will be assumed to

have length L , tension T , mass per unit length ρ and bending rigidity B . (For a homogeneous solid string of radius a and Young’s modulus E , $B = E\pi a^4/4$.) In the simplest case, the string undergoes transverse vibration in a single plane normal to the guitar’s soundboard, with transverse displacement $y(x, t)$ at position x and time t . At one end, $x = 0$ say, the string is assumed for the moment to be rigidly anchored so that it has no displacement. At the other end, $x = L$, it is attached to the body of the guitar so that string and body have identical displacements. If string vibration with both polarisations is included, transverse displacement $z(x, t)$ will be assumed in the plane parallel to the guitar’s soundboard.

For the body, the most direct characterisation of dynamic behaviour is via the input admittance at the point on the bridge where the string makes contact, or more generally via the admittance matrix at this point. We may choose to process this admittance to extract modal properties: each mode has an effective mass, effective stiffness, damping factor, and angle of movement at the bridge. It also has a radiation efficiency and pattern, which would be relevant if the desire was to synthesise the sound field. However, the emphasis here will be on predicting the transient response measured on the *structure*. So far as this paper is concerned, sound radiation is relevant only as one mechanism contributing to the modal damping factors. Other effects of the air around the guitar body are included implicitly: they influence the input admittance, and the “modes” into which this may be decomposed are the coupled air-structure modes. It will be seen that this sub-problem is already quite challenging, without the additional layer of difficulties associated with radiation and room acoustics.

The relation between input admittance (velocity per unit force) $Y(\omega)$ of the body at the string’s attachment point and the modal properties is given by the standard formula (see for example Skudrzyk [12])

$$Y(\omega) = \sum_k \frac{i\omega}{m_k(\omega_k^2 + i\omega\omega_k\eta_k - \omega^2)}, \quad (1)$$

where ω is the angular frequency, and the k th mode of vibration of the body (including the surrounding air) in the absence of the strings has effective mass m_k , natural frequency ω_k and modal damping factor η_k (or corresponding modal Q -factor $Q_k = 1/\eta_k$). The “effective mass” is related directly to the k th mode shape u_k : if the mode shape is normalised in the usual way with respect to the system mass matrix [11], then

$$m_k = 1/u_k^2 \text{ (bridge)}, \quad (2)$$

where (bridge) connotes the attachment point of the string. At least for the moment, the mode shapes, and hence the effective masses, will be assumed to be real: in other words, proportional damping is assumed for the body vibration. Damping will also be assumed to be small, so that $\eta_k \ll 1$ or $Q_k \gg 1$. Very similar expressions to equation (1) hold for the more general case of the 2×2 admittance matrix at the bridge, which is needed when both

string polarisations are included in the synthesis model. Details of this case are given in section 3.3. (Note that the expression (1) appears at first sight to be different in form to the expression for admittance given by Christensen and Vistisen [13, equation(6a)], which takes explicit account of the structure and the enclosed air. However, if the denominator of their expression is factorised and the whole expression then expanded in partial fractions, it takes the form (1) above.)

2.2. Modal synthesis

The first class of synthesis methods works by computing the coupled string/body modes, together with appropriate frequencies and damping factors, then using modal superposition to construct the transient response. This could be the response to an idealised pluck, a step function of force applied at a single point of the string, or more generally it could be the response to any given patterns of initial displacement and velocity: for example, the low-pass filtering effect associated with the finite stiffness and radius of curvature of the player's fingertip could be included (see for example Benade [14, chapter 8]).

The simplest modal approach proceeds in four stages. First, a suitable set of generalised coordinates is chosen to describe the motion of the string and body, and the mass and stiffness matrices for the coupled system are worked out in terms of these generalised coordinates. For the present purpose, the most natural choice of generalised coordinates consists of (i) the mode amplitudes of the body in the absence of strings; (ii) a set of Fourier series coefficients for the string displacement, in other words the amplitudes of what would be the string modes if both ends of the string were rigidly fixed; and (iii) one or two "constraint modes" (see e.g. [9]), to allow the string to move at the end attached to the body. The resulting mass and stiffness matrices will be calculated in detail in section 3.1. In the second stage of the pluck calculation, the modes and natural frequencies of the coupled string/body system are computed in the absence of damping by standard eigenvalue/eigenvector analysis. Third, a suitable Q -factor is calculated for each mode using a small-damping argument based on Rayleigh's principle [15, 16]. Finally, the transient response to an ideal pluck at a given position on the string can be calculated using a standard modal superposition result: again, details are given in section 3.1.

The method just outlined is precisely what is used in the vast majority of calculations of the vibration response of complex structures. For example, almost all Finite-Element calculations work this way (although they usually use a cruder estimate of modal damping than that resulting from the Rayleigh's quotient method). Unfortunately, as pointed out by Gough [6], this method does not always give a good approximation to the correct answer. The crucial issue concerns what is usually called "veering" behaviour [17]. Imagine adjusting the tuning of the string so that one particular string overtone passes close to the frequency of a body mode. At the point where the string and body resonant frequencies were expected to co-

incide, the undamped modal calculation will always produce two separated frequencies, with the two corresponding coupled modes involving significant motion of both string and body, in phase for one mode and in antiphase for the other. The Rayleigh calculation of modal damping factors will assign both modes equal damping at this "tuned" point. This effect, giving relatively high damping to both modes when playing a note very close to a strong body resonance, is often described by guitar players with a phrase like "this note falls flat". However, the intrinsic internal damping of the string mode will generally be far lower than that of the body mode, and under these circumstances Gough shows that the correct result may be very different from that just described. If the disparity of damping between the string and the body is large compared to a measure of the strength of coupling between string and body, then when the string mode is tuned through the frequency of the body mode, behaviour is seen similar to that illustrated in Figure 1. Figure 1(a) shows the variation of the two modal frequencies through the "tuning" range. The frequencies calculated ignoring damping show "veering" behaviour, but the correct frequencies allowing for the effects of damping cross over. Figure 1(b) shows the corresponding behaviour of the modal loss factors. When calculated by the Rayleigh argument based on undamped modes, the two curves cross so that at the "tuned" condition the damping factors are equal. In the correct calculation, by contrast, the two damping factors remain very different throughout the range, so that it is always possible to identify one "string" mode with low damping and one "body" mode with higher damping. The key to the difference in behaviour is that the mode shapes become significantly complex in the correct calculation, invalidating the assumption underlying the Rayleigh method. The detailed calculation leading to this figure will be described in section 3.4.

To avoid the problem just illustrated, it is necessary to tackle the rather murky question of how the damping of the string/body system should be modelled, so that realistic modal behaviour of the coupled, damped system can be calculated. Unfortunately, there is no universal damping model which has the same physical credibility as the standard models of elastic and inertial effects through the stiffness and mass matrices. When an explicit damping model is needed, it is conventional to use the "viscous damping model" first introduced by Rayleigh [18]. If it is assumed that the rate of energy dissipation depends only on the instantaneous values of the generalised velocities, then for small motions it is reasonable to approximate this dissipation rate by a quadratic expression in the velocities, and thus introduce a third matrix, the *dissipation matrix* C , so that the equations of free motion of the system take the form

$$M\ddot{\mathbf{q}} + C\dot{\mathbf{q}} + K\mathbf{q} = 0, \quad (3)$$

where \mathbf{q} is the vector of generalised coordinates, and M and K are the mass and stiffness matrices respectively. Whether and when it is acceptable to use this viscous

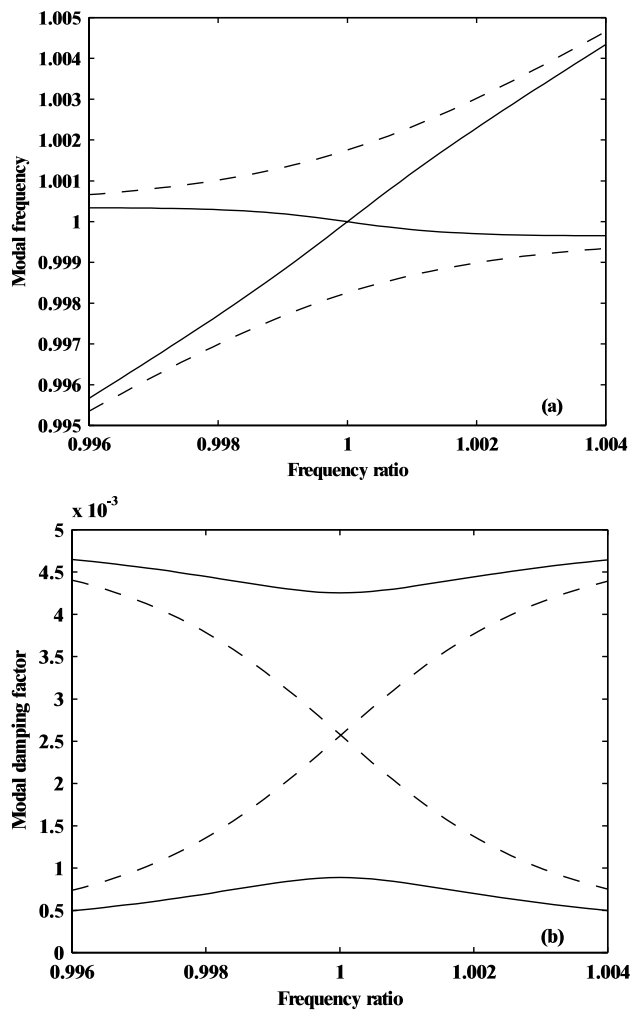


Figure 1. Veering and non-veering behaviour in a simple model of one string mode coupled to one body mode. The uncoupled body mode has a fixed frequency and a Q -factor of 100, while the uncoupled string mode has a Q -factor of 3500 and a frequency varying over a small range. The variation of (a) the coupled mode frequencies and (b) the modal damping factors is plotted against the frequency ratio of the two uncoupled modes. The dashed lines show “veering” behaviour, when the calculation is based on undamped modes followed by Rayleigh’s principle to determine modal damping, while the solid line uses the first-order method to find damped modes directly and shows “non-veering” behaviour. The detailed theory is given in section 3.4

model of damping is a subject of some debate (see for example [19, 20]). It will be used provisionally in this study, but it should be kept in mind that experimental results may require the issue to be revisited in the future.

In the undamped problem, it is always possible to reduce M and K to diagonal form by using the modal amplitudes as new generalised coordinates. With three matrices M , C and K , it is not possible to diagonalise all three simultaneously by using modal coordinates. It is therefore common to introduce a further approximation at this point, so-called “proportional damping”. Since information about C for real systems is usually rather sketchy, it may be assumed that it is diagonalised simultaneously

with M and K by the usual (real) mode shapes. There are some mathematical conditions under which this is justified (see Caughey [21]), but there is rarely any reason to expect these conditions to hold for a physical system. Proportional damping is simply a mathematically convenient assumption, which usually works well enough. In the string/body coupling problem, Gough’s result shows that we cannot make this assumption.

To retain a “modal” approach while solving equations (3) with a non-proportional damping matrix C , the usual method is to recast the equations into first-order form. This can be done in more than one way, but the most direct is to define a double-length vector

$$p = \begin{bmatrix} q \\ \dot{q} \end{bmatrix}, \quad (4)$$

and a $2N \times 2N$ matrix

$$A = \begin{bmatrix} 0 & I \\ -M^{-1}C & -M^{-1}K \end{bmatrix}, \quad (5)$$

where 0 denotes the $N \times N$ zero matrix and I the $N \times N$ unit matrix, N being the number of degrees of freedom. The equations (3) can then be rewritten

$$\dot{p} = Ap. \quad (6)$$

Now a modal solution $p(t) = v_k e^{\lambda_k t}$ leads to

$$Av_k = \lambda_k v_k. \quad (7)$$

Solving this eigenvalue/eigenvector problem yields the (complex) mode vectors and associated complex natural frequencies, and there are then standard formulae for frequency response functions and impulse response functions in terms of modal sums (see for example Newland [22, chapter 8]).

In summary, there are two types of modal synthesis which could be used for guitar plucks. One is based on undamped modes, post-processed to give damping factors, while the other uses the first-order approach to give damped modes directly (assuming a viscous model for damping in the whole system). The first of these is simpler and involves smaller matrices, but may give wrong answers under some circumstances. The second is more accurate, but at the cost of doubling the size of the eigenproblem to be solved. Both methods share certain advantages over some other methods to be discussed shortly. First, they work in terms of degrees of freedom which are very natural: loosely, “string mode amplitudes” and “body mode amplitudes”. This is very convenient for parametric studies; for example, to explore the influence on sound quality of particular body mode frequencies and damping factors. A second advantage is that once the modes have been computed, the desired transient response is given by an explicit formula which introduces no further approximations or numerical difficulties. If a calculation of the radiated sound is wanted, the modal formulation is again convenient: the modal sum expressing the transient response simply has to be weighted by factors describing the modal radiation strengths (e.g. [23, 24]).

A disadvantage of these methods is that they require the body response to be expressed in terms of modal properties over the entire frequency range. This is simple and natural at low frequencies, but by frequencies of the order of 1 kHz in a typical classical guitar the modal overlap factor of the body starts to become significant, and above that it is neither easy nor unambiguous to extract modal parameters from a measured admittance.

2.3. Frequency domain synthesis

A completely different approach to the synthesis problem is to deal with the string/body coupling in the frequency domain, and then use an inverse FFT to create the required time-varying transient response. This method is attractive because the string and the body are coupled together at a single point, and there is a very simple method which can be applied to any such problem: if two systems have input admittances $Y_1(\omega)$ and $Y_2(\omega)$ and they are then rigidly connected at the points at which these admittances are defined, then the coupled system has an admittance Y at that point satisfying

$$\frac{1}{Y} = \frac{1}{Y_1} + \frac{1}{Y_2}. \quad (8)$$

This result expresses the fact that at the coupling point, the two subsystems have equal velocities while the total applied force is the sum of the forces applied to the two separate subsystems. In the more general case in which the coupling applies to more than one direction of motion, then an equivalent result applies to the relevant admittance matrices:

$$Y^{-1} = Y_1^{-1} + Y_2^{-1}. \quad (9)$$

The body is naturally described in terms of its admittance (or admittance matrix), as already described. By calculating the corresponding admittance at the end of a string, which will be derived in section 3.2, these results can be applied immediately to give the impedance or impedance matrix of the strung guitar at the bridge.

To use this method to derive a pluck response, use can be made of the reciprocal theorem of vibration response. We wish to find the body vibration which results from a step function of force applied at a given position on the string. Reciprocally, we can consider applying the force at the bridge, and calculate the resulting motion at the relevant point on the string (and in the relevant direction there, if string polarisations are to be taken into account). To solve this reciprocal problem, we simply have to multiply two transfer functions together. The first is the coupled admittance just calculated, which gives the velocity at the bridge when a force is applied there. The second is the dimensionless transfer function between a given displacement applied at one end of a string and the corresponding displacement at the point where the pluck is to be applied. This second transfer function is also derived in section 3.2.

The advantages of this frequency-domain approach are that it is very simple, and that it gives the choice of expressing the body admittance in terms of modes, as before,

or of using the measured admittance directly, thus avoiding the complication of modal fitting at high frequencies. A potential disadvantage of the method is its reliance on inverse Fourier transformation at the final stage. Given the inevitable discrete frequency resolution and finite bandwidth it is hard to guarantee an answer which is absolutely causal. However, it will be seen in section 4 that a sufficiently causal result can be achieved, and that makes this method very attractive.

Finally, it should be noted that there is a completely different approach to frequency-domain synthesis based on equation (3). By adding a vector of appropriate generalised forces on the right-hand side of this equation and then taking the Fourier transform, it is clear that the matrix of transfer functions can be derived directly by inverting the so-called “dynamic stiffness matrix”

$$D = -\omega^2 M + i\omega C + K. \quad (10)$$

Using the same expressions for M , C and K as are needed for modal synthesis, this inversion can be carried out frequency by frequency, then the relevant transfer function extracted from the matrix, and an inverse FFT performed to give the transient response. This method has the virtue of great conceptual simplicity, but in practice it is extremely slow. The method is useful as a cross-check on the coding of other methods, but is not a serious contender for an efficient synthesis algorithm.

2.4. Time domain synthesis

Finally, there is a class of possible synthesis methods which work directly in the time domain. Two such methods can be found in the existing literature: to use a finite-difference approach to integrate directly the differential equation governing string motion [25], or to adapt the synthesis method used in bowed-string studies, the so-called “digital waveguide” approach (see for example [10, 26]). The finite-difference method starts from the differential equations for the string and body motion. The various derivatives are approximated by difference formulae, and the result is a formulation which lends itself to forward integration by time marching. However, to apply such a method to the model which will be used here, including such effects as string bending stiffness, frequency-dependent damping and accurate body modes up to at least 5 kHz, would require a level of detail in the implementation which goes well beyond published work, and probably poses significant challenges of accuracy and speed, so this approach will not be explored further here.

The digital waveguide approach is mathematically closely related to the finite-difference method, but expressed in a more flexible and versatile form which does not rely on underlying differential equations. The various physical effects from the strings and the body are taken into account via “reflection functions”, essentially impulse responses which encapsulate the various processes of dissipation, dispersion and reflection which occur as a wave travels back and forth along the string. Any process which

can be represented by a digital filter of some kind can be incorporated.

Earlier bowed-string studies have provided almost all the ingredients necessary to attempt a synthesis of a guitar pluck comparable to those possible by the other methods already mentioned. The basic behaviour of transverse waves on an ideal string is handled directly by the digital waveguide method. The dispersive effect of bending stiffness in the string can be handled using a reflection function reported by Woodhouse [27], and this has been shown to work well to reproduce the pluck response of a violin E string held by relatively rigid terminations [28]. For a trial of the method, internal damping in the string can be handled using a “constant- Q ” reflection function [29]. Frequency-dependent string damping could in principle be incorporated by designing a suitable digital filter. Body resonances can be incorporated via a suitable reflection function based on the impulse response of the body [30]. Using the modal properties of the body input admittance, this can be efficiently implemented using recursive IIR digital filters, one per mode (see for example [31]). Bowed-string studies have not generally considered the second polarisation of string motion, but there is no difficulty in principle in incorporating this into the model. In short, existing algorithms can be assembled to give a time-domain synthesis method for a guitar pluck which addresses the same physical phenomena which will be included in the other methods.

However, the results of a test case were disappointing. In section 4, the results will be shown of syntheses by various of the methods described above, using a standard set of parameters: 6 seconds of synthesis, a sampling rate of 22050 Hz, and enough string and body modes to cover the range up to 5 kHz. At this sampling rate, the digital waveguide synthesis as described above proved to have poor accuracy, and more seriously it frequently resulted in unstable, growing behaviour when trying to cope with the rather low inherent damping of guitar strings. This instability had its origin in problems with the “stiff string” reflection function, with appropriate parameter values for classical guitar strings. None of the other methods described earlier have the possibility of instability in this sense. These faults can be corrected, mainly by using a higher sampling rate. Equally, different digital filters could no doubt be designed to improve matters, as has been done in work aimed at musical synthesis (e.g. [10]). However, in the implementation used here and in comparison with other methods presented, this method does not offer an accurate and efficient synthesis method for guitar plucks for “laboratory” purposes, and it will not be considered further here.

3. Implementation details

In this section a number of technical aspects of the synthesis algorithms are dealt with, in order that explicit implementations of various candidate methods can be made. The results of these are then compared with each other in section 4, and with experimental measurements in a companion paper [1].

3.1. Computing the coupled modes

All the modal methods require the mass, stiffness and damping matrices for the coupled string/body system. These are derived here for the case of a single polarisation of string vibration. The extension to include two polarisations is dealt with in section 3.3. A convenient and simple approach to the problem is to use Rayleigh’s principle based on three sets of generalised coordinates: the modes of the string with pinned ends, the modes of the unstrung body as experienced through the coupling point at the bridge, and one “constraint mode” which is the static response of the string when the end at the bridge is allowed to move [9]. Accordingly, write the string displacement in the form

$$y(x) = a_0 \frac{x}{L} + \sum_{j=1}^{N_s} a_j \sin \frac{j\pi x}{L}, \quad (11)$$

where the quantities a_0 , a_j are the (time-dependent) amplitudes of the constraint mode and the j th pinned string mode respectively, and N_s is the number of string modes used in the calculation. (Pinned boundary conditions for the string in isolation seem appropriate, even in the presence of bending stiffness, because of the “crossed cylinder” geometry of a string over a fret or over the bridge saddle.) Similarly, denote the amplitude of motion at the bridge of the k th body mode by b_k . For the string and body motion to be equal at the point $x = L$,

$$a_0 = \sum_{k=1}^{N_b} b_k, \quad (12)$$

where N_b is the number of body modes used in the calculation.

The total potential energy of the system is then

$$V = \frac{1}{2} \sum_{k=1}^{N_b} s_k b_k^2 + \frac{1}{2} T \int_0^L \left(\frac{\partial y}{\partial x} \right)^2 dx + \frac{1}{2} B \int_0^L \left(\frac{\partial^2 y}{\partial x^2} \right)^2 dx, \quad (13)$$

where the three terms arise respectively from the stored energy in the body resonances, the energy in the string due to tension effects, and the energy in the string due to bending stiffness effects. The terms s_k denote the effective stiffnesses of the body modes, defined by

$$s_k = m_k \omega_k^2. \quad (14)$$

Substituting equation (11), eliminating a_0 using (12) and evaluating the integrals leads to

$$V = \frac{1}{2} \sum_{k=1}^{N_b} s_k b_k^2 + \frac{1}{2} \frac{T}{L} \left[\sum_{k=1}^{N_b} b_k \right]^2 + \frac{1}{2} \frac{T\pi^2}{2L} \sum_{j=1}^{N_s} j^2 a_j^2 + \frac{1}{2} \frac{B\pi^4}{2L^3} \sum_{j=1}^{N_s} j^4 a_j^2, \quad (15)$$

from which the stiffness matrix may be immediately deduced. In terms of the coordinate vector

$$\mathbf{q} = [a_1, a_2, a_3, \dots, b_1, b_2, \dots]^t \quad (16)$$

it is given by

$$\mathbf{K} = \begin{bmatrix} K_{11} & 0 \\ 0 & K_{22} \end{bmatrix},$$

where

$$K_{11} = \text{diag} \left\{ \frac{T\pi^2}{2L} + \frac{B\pi^4}{2L^3}, \frac{4T\pi^2}{2L} + \frac{16B\pi^4}{2L^3}, \dots, \frac{j^2 T\pi^2}{2L} + \frac{j^4 B\pi^4}{2L^3}, \dots \right\}$$

and

$$K_{22} = \begin{bmatrix} s_1 + T/L & T/L & \dots & T/L & \dots \\ T/L & s_2 + T/L & & & \\ \vdots & & \ddots & & \\ T/L & & & s_k + T/L & \\ \vdots & & & & \ddots \end{bmatrix}. \quad (17)$$

In a similar way, the total kinetic energy of the system is $-\omega^2 \tilde{T}$ where

$$\begin{aligned} \tilde{T} &= \frac{1}{2} \sum_{k=1}^{N_b} m_k b_k^2 + \frac{1}{2} \rho \int_0^L y^2 dx \\ &= \frac{1}{2} \sum_{k=1}^{N_b} m_k b_k^2 + \frac{1}{2} \frac{\rho L}{3} \left[\sum_{k=1}^{N_b} b_k \right]^2 + \frac{1}{2} \frac{\rho L}{2} \sum_{j=1}^{N_s} a_j^2 \\ &\quad - \frac{1}{2} \frac{2\rho L}{\pi} \left(\sum_{k=1}^{N_b} b_k \right) \left(\sum_{j=1}^{N_s} \frac{(-1)^j a_j}{j} \right), \quad (18) \end{aligned}$$

from which the mass matrix may be written down:

$$\mathbf{M} = \begin{bmatrix} M_{11} & M_{12} \\ M_{12}^t & M_{22} \end{bmatrix},$$

where

$$M_{11} = \text{diag} \{ \rho L/2, \rho L/2, \dots, \rho L/2, \dots \},$$

$$M_{12} = \begin{bmatrix} \rho L/\pi & \rho L/\pi & \dots & \rho L/\pi & \dots \\ -\rho L/2\pi & -\rho L/2\pi & \dots & -\rho L/2\pi & \dots \\ \vdots & & & & \\ (-1)^{j+1} \frac{\rho L}{j\pi} & (-1)^{j+1} \frac{\rho L}{j\pi} & \dots & (-1)^{j+1} \frac{\rho L}{j\pi} & \dots \\ \vdots & & & & \vdots \end{bmatrix}$$

and

$$M_{22} = \begin{bmatrix} m_1 + \frac{\rho L}{3} & \frac{\rho L}{3} & \dots & \frac{\rho L}{3} & \dots \\ \frac{\rho L}{3} & m_2 + \frac{\rho L}{3} & & & \\ \vdots & & \ddots & & \\ \frac{\rho L}{3} & & & m_k + \frac{\rho L}{3} & \\ \vdots & & & & \ddots \end{bmatrix}. \quad (19)$$

As is usual with a “constraint mode” formulation, the stiffness matrix has no string/body coupling terms: these occur only in the mass matrix (in submatrix M_{12}) [9].

The next requirement is to specify the associated damping behaviour. The simplest possible model will be taken. Each body mode and each string mode (in the absence of body coupling) will be assigned an individual modal Q -factor. In practice, the body damping factors are determined as part of the process of modal fitting to measured admittance behaviour, while the string damping factors will follow a systematic trend with frequency of the kind measured by Valette [3]. Notice, though, that an assumption underlies this apparently obvious damping model: by specifying only “modal damping factors”, proportional damping is implicitly being assumed for the string and the body considered in isolation. In the light of the earlier comments about the dubious justification for any assumption of proportional damping this may seem a little odd. However, it seems to be the only realistic assumption at the present time, given the difficulty of obtaining reliable experimental data on non-proportionally damped systems. This is an issue to which it may be necessary to return in the future: for example, the “body modes” used here are in reality coupled air/body modes, and it is possible that this coupling may lead to significantly complex modes, and also to complex “modal masses” in the formulation used here.

Two different methods for incorporating damping into modal synthesis of the coupled string–body system were described in section 2.2: via post-processing of the undamped modes using Rayleigh’s principle, and via a viscous damping matrix \mathbf{C} . For the Rayleigh method, the expression for the total potential energy (13) of the string and body is modified by replacing the tension, bending rigidity and effective stiffnesses of the body modes by complex values embodying the desired Q -factors:

$$\begin{aligned} T &\longrightarrow T(1 + i/Q_T), \\ B &\longrightarrow B(1 + i/Q_B), \\ s_k &\longrightarrow s_k(1 + i/Q_k). \end{aligned} \quad (20)$$

The damping factors associated with the tension and the bending rigidity can vary with the frequency of the mode in question if desired. The Rayleigh quotient incorporating these complex constants but evaluated using the undamped mode vector as a trial function gives an approximation to the complex frequency of the damped system [16], and hence the Q -factor of the coupled string/body mode in question:

$$\frac{1}{Q_n} \approx \frac{\Im m\{\omega_n^2\}}{\Re e\{\omega_n^2\}} \approx \frac{\mathbf{u}_n^t \mathbf{K}' \mathbf{u}_n}{\mathbf{u}_n^t \mathbf{K} \mathbf{u}_n}, \quad (21)$$

where

$$\mathbf{K}' = \begin{bmatrix} K'_{11} & 0 \\ 0 & K'_{22} \end{bmatrix},$$

with

$$K'_{11} = \text{diag} \left\{ \frac{T\pi^2}{2LQ_T} + \frac{B\pi^4}{2L^3Q_B}, \frac{4T\pi^2}{2LQ_T} + \frac{16B\pi^4}{2L^3Q_B}, \dots, \frac{j^2T\pi^2}{2LQ_T} + \frac{j^4B\pi^4}{2L^3Q_B}, \dots \right\}$$

and

$$K'_{22} = \begin{bmatrix} \frac{s_1}{Q_1} + \frac{T}{LQ_T} & \frac{T}{LQ_T} & \dots & \frac{T}{LQ_T} & \dots \\ \frac{T}{LQ_T} & \frac{s_2}{Q_2} + \frac{T}{LQ_T} & & & \\ \vdots & & \ddots & & \\ \frac{T}{LQ_T} & & & \frac{s_k}{Q_k} + \frac{T}{LQ_T} & \\ \vdots & & & & \ddots \end{bmatrix} \quad (22)$$

For the viscous damping model, the dissipation matrix takes the simple diagonal form

$$C = \begin{bmatrix} C_{11} & 0 \\ 0 & C_{22} \end{bmatrix},$$

where

$$C_{11} = \frac{\pi\sqrt{T\rho}}{2} \text{diag} \left\{ \frac{1}{Q_{s1}}, \frac{2}{Q_{s2}}, \dots, \frac{j}{Q_{sj}}, \dots \right\},$$

$$C_{22} = \text{diag} \left\{ \frac{\sqrt{s_1 m_1}}{Q_1}, \frac{\sqrt{s_2 m_2}}{Q_2}, \dots, \frac{\sqrt{s_k m_k}}{Q_k}, \dots \right\}, \quad (23)$$

and Q_{sj} is the Q -factor of the j th string mode.

This completes the information needed to calculate the coupled modes, either undamped or damped. The calculation of the response to an ideal pluck at position x is then simple. In the first case, suppose that the undamped modes \mathbf{u}_n and natural frequencies ω_n have been calculated from M and K , and the appropriate modal Q factors Q_n determined from equation (21). Each mode should be normalised so that

$$\mathbf{u}_n^t M \mathbf{u}_n = 1.$$

A standard formula for impulse response can now be used. Note that the velocity response of the body to an impulse applied to the string will be the same as the acceleration response of the body to a step function force applied at the same point. This acceleration response is then given by

$$g(t) = \sum_{n=1}^N \alpha_n \beta_n \cos(\omega_n t) e^{-\omega_n t / 2Q_n}, \quad (24)$$

where

$$\alpha_n = \sum_k b_k^{(n)}$$

is the modal motion at the bridge from equation (12), where $b_k^{(n)}$ denotes the value of b_k appropriate to the n th mode, and

$$\beta_n = \alpha_n x / L + \sum_{j=1}^{N_s} a_j^{(n)} \sin(j\pi x / L)$$

is the corresponding motion at the plucking point x from equation (11), where $a_k^{(n)}$ denotes the value of a_k appropriate to the n th mode.

A similar modal sum can be used if damped modes and frequencies have been calculated using the first-order form:

$$g(t) = \sum_{n=1}^{2N} \gamma_n \beta_n e^{\lambda_n t}, \quad (25)$$

where β_n is as above, and

$$\gamma_n = \sum_{k=N_s+1}^N X_{nk}, \quad \text{where} \quad X = V_{\text{right}}^{-1} M^{-1}$$

and V_{right}^{-1} is the $2N \times N$ matrix which is the right-hand half of the inverse of the matrix whose columns are the eigenvectors of the matrix A : see [22, equation (8.110) et seq.].

3.2. Frequency response functions of the string

The frequency-domain synthesis methods require as input the drive-point impedance at the end of the string, and also the transfer function linking motion at the end to motion at the required plucking point. For the case of an ideal, undamped string there are analytic formulae for both. However, the effects of bending stiffness and, more importantly, string damping are essential to an accurate synthesis. To include these effects, one simple approach is to expand the analytic expressions in partial fractions, interpret the terms as corresponding to the modes of the string, then adjust the complex pole frequencies to allow for stiffness and damping. The residues associated with these poles are kept unchanged – this amounts to the same approximation as assuming that the string in isolation has proportional damping.

Suppose the string is fixed at position $x = 0$, and that a harmonic displacement $w e^{i\omega t}$ is imposed at $x = L$. To satisfy the fixed boundary condition, the string displacement must take the form

$$y = a \sin \omega x / c,$$

where a is a constant and $c = \sqrt{T/\rho}$ is the wave speed on the string. Imposing the other boundary condition fixes the value of a , so that the response is

$$y = w \frac{\sin \omega x / c}{\sin \omega L / c}. \quad (26)$$

Now if the end motion is caused by a force $f e^{i\omega t}$ applied to the string, force balance requires

$$f = T \frac{\partial y}{\partial x} \Big|_{x=L} = \frac{T w \omega \cos \omega L / c}{c \sin \omega L / c},$$

so the required end impedance is

$$Z = \frac{f}{i\omega w} = \frac{T}{ic} \cot \frac{\omega L}{c} = -iZ_0 \cot \frac{\omega L}{c}, \quad (27)$$

where Z_0 is the characteristic impedance of the string.

The impedance Z has poles at $\omega L/c = n\pi$, $n = 0, \pm 1, \pm 2, \dots$. It is readily shown that all poles have the same residue $-iT/L$, so

$$Z = -\frac{iT}{L} \sum_{n=-\infty}^{\infty} \frac{1}{\omega - n\pi c/L}. \quad (28)$$

The corresponding expression with (small) modal damping included is

$$Z = -\frac{iT}{L} \left[\frac{1}{\omega} + \sum_{j=1}^{\infty} \left\{ \frac{1}{\omega - \omega_j(1 + i\eta_{sj}/2)} + \frac{1}{\omega + \omega_j(1 - i\eta_{sj}/2)} \right\} \right] \\ \approx -\frac{iT}{L} \left[\frac{1}{\omega} + \sum_{j=1}^{\infty} \left\{ \frac{2\omega - i\omega_j\eta_{sj}}{\omega^2 - i\omega\omega_j\eta_{sj} - \omega_j^2} \right\} \right], \quad (29)$$

where $\eta_{sj} = 1/Q_{sj}$ is the loss factor of the j th string mode. The modal frequency can be adjusted to allow for small bending stiffness in the string by setting

$$\omega_j \approx \frac{i\pi c}{L} \left[1 + \frac{B}{2T} \left(\frac{j\pi}{L} \right)^2 \right], \quad (30)$$

a result which follows from Rayleigh's principle applied to the string terms of equation (13). A similar procedure can be applied to equation (26) to provided a damped approximation to the transfer function from the end of the string to the plucking point:

$$\frac{y}{w} \approx \frac{x}{L} + \frac{c}{L} \sum_{j=1}^{\infty} (-1)^j \frac{2\omega \sin j\pi x/L}{\omega^2 - i\omega\omega_j\eta_{sj} - \omega_j^2}. \quad (31)$$

Note that equations (29) and (31) both give the correct static response: when $\omega = 0$ the string deflects in a straight line, the same shape used earlier as the "constraint mode", and the impedance is then spring-like with a stiffness T/L .

Note in passing that equations (29) and (31) could also be derived by a different approach, which is commonly used in earthquake engineering (e.g. [32]). Starting from the expression (11), the applied end displacement can only drive directly the motion described by the constraint mode. That motion has associated with it an inertial reaction force (a "d'Alembert force") distributed along the string, which can be resolved into components driving the other modes of the string, leading to expressions for the desired transfer functions.

3.3. String polarisations

The modal and frequency-domain synthesis methods can be readily extended to include two polarisations of string motion. At the bridge, motion normal and parallel to the soundboard has to be taken into account, so in place of the input admittance Y there is a matrix. It is convenient to define Y_{11} to be the previous admittance in the normal direction, so that Y_{22} is the admittance in the direction

parallel to the bridge saddle, and Y_{12} is the cross admittance. As before, these can be expressed in terms of body modes. However, we now need an additional property of each mode: the angle θ_k of the body motion at the bridge measured from the normal direction. Then

$$Y_{11}(\omega) = \sum_k \frac{i\omega \cos^2 \theta_k}{m_k(\omega_k^2 - i\omega\omega_k\eta_k - \omega^2)},$$

$$Y_{22}(\omega) = \sum_k \frac{i\omega \sin^2 \theta_k}{m_k(\omega_k^2 - i\omega\omega_k\eta_k - \omega^2)},$$

and

$$Y_{12}(\omega) = Y_{21}(\omega) = \sum_k \frac{i\omega \cos \theta_k \sin \theta_k}{m_k(\omega_k^2 - i\omega\omega_k\eta_k - \omega^2)}. \quad (32)$$

This is all that is needed for frequency-domain synthesis via equation (8), except to note that the string behaviour is rotationally symmetric so that the corresponding impedance matrix is simply the impedance Z from equation (29) multiplied by a 2×2 unit matrix.

For modal synthesis, it is necessary to introduce a second constraint mode, identical in form to the first but in the plane parallel to the soundboard. Then express the string motion in that plane analogous to equation (11), as

$$z(x) = a'_0 \frac{x}{L} + \sum_{j=1}^{N_s} a'_j \sin \frac{j\pi x}{L}, \quad (33)$$

where the quantities a'_0, a'_j are the equivalents of a_0, a_j for this plane. Now from continuity of displacement at the bridge,

$$a_0 = \sum_{k=1}^{N_b} b_k \cos \theta_k, \quad a'_0 = \sum_{k=1}^{N_b} b_k \sin \theta_k, \quad (34)$$

in place of equation (12). The calculation of kinetic and potential energies then follows very similar lines, except that the term $[\sum b_k]^2$ is replaced by

$$\left[\sum b_k \cos \theta_k \right]^2 + \left[\sum b_k \sin \theta_k \right]^2 \\ = \sum_k \sum_l b_k b_l \cos(\theta_k - \theta_l). \quad (35)$$

In terms of an extended vector of generalised coordinates

$$\mathbf{q} = [a_1, a_2, a_3, \dots, a'_1, a'_2, a'_3, \dots, b_1, b_2, \dots]^t, \quad (36)$$

the result for the stiffness matrix is

$$K = \begin{bmatrix} K_{11} & 0 & 0 \\ 0 & K_{11} & 0 \\ 0 & 0 & K_{33} \end{bmatrix},$$

where K_{11} is as before and

$$K_{33} = \begin{bmatrix} s_1 + \frac{T}{L} & \frac{\cos(\theta_1 - \theta_2)T}{L} & \dots & \frac{\cos(\theta_1 - \theta_k)T}{L} & \dots \\ \frac{\cos(\theta_1 - \theta_2)T}{L} & s_2 + \frac{T}{L} & & & \\ \vdots & & \ddots & & \\ \frac{\cos(\theta_1 - \theta_k)T}{L} & & & s_k + \frac{T}{L} & \\ \vdots & & & & \ddots \end{bmatrix}. \quad (37)$$

The mass matrix is given by

$$M = \begin{bmatrix} M_{11} & 0 & M_{13} \\ 0 & M_{11} & M_{23} \\ M_{13}^t & M_{23}^t & M_{33} \end{bmatrix},$$

where M_{11} is as before,

$$M_{13} = \begin{bmatrix} \frac{\cos \theta_1 \rho L}{2\pi} & \frac{\cos \theta_2 \rho L}{2\pi} & \dots \\ -\frac{\cos \theta_1 \rho L}{2\pi} & -\frac{\cos \theta_2 \rho L}{2\pi} & \dots \\ \vdots & \vdots & \ddots \\ (-1)^{j+1} \frac{\cos \theta_1 \rho L}{j\pi} & (-1)^{j+1} \frac{\cos \theta_2 \rho L}{j\pi} & \dots \\ \vdots & \vdots & \ddots \\ \dots & \frac{\cos \theta_j \rho L}{2\pi} & \dots \\ \dots & -\frac{\cos \theta_j \rho L}{2\pi} & \dots \\ \vdots & \vdots & \ddots \\ \dots & (-1)^{j+1} \frac{\cos \theta_j \rho L}{j\pi} & \dots \\ \vdots & \vdots & \ddots \end{bmatrix},$$

$$M_{23} = \begin{bmatrix} \frac{\sin \theta_1 \rho L}{2\pi} & \frac{\sin \theta_2 \rho L}{2\pi} & \dots \\ -\frac{\sin \theta_1 \rho L}{2\pi} & -\frac{\sin \theta_2 \rho L}{2\pi} & \dots \\ \vdots & \vdots & \ddots \\ (-1)^{j+1} \frac{\sin \theta_1 \rho L}{j\pi} & (-1)^{j+1} \frac{\sin \theta_2 \rho L}{j\pi} & \dots \\ \vdots & \vdots & \ddots \\ \dots & \frac{\sin \theta_j \rho L}{2\pi} & \dots \\ \dots & -\frac{\sin \theta_j \rho L}{2\pi} & \dots \\ \vdots & \vdots & \ddots \\ \dots & (-1)^{j+1} \frac{\sin \theta_j \rho L}{j\pi} & \dots \\ \vdots & \vdots & \ddots \end{bmatrix},$$

and

$$M_{33} = \begin{bmatrix} m_1 + \frac{\rho L}{3} & \frac{\cos(\theta_1 - \theta_2) \rho L}{3} & \dots & \frac{\cos(\theta_1 - \theta_k) \rho L}{3} & \dots \\ \frac{\cos(\theta_1 - \theta_2) \rho L}{3} & m_2 + \frac{\rho L}{3} & & & \\ \vdots & & \ddots & & \\ \frac{\cos(\theta_1 - \theta_k) \rho L}{3} & & & m_k + \frac{\rho L}{3} & \\ \vdots & & & & \ddots \end{bmatrix}. \quad (38)$$

If the assumption of proportional damping for the string and body separately is retained, then the matrices K' and C may be obtained by simple extension of the earlier results:

$$K' = \begin{bmatrix} K'_{11} & 0 & 0 \\ 0 & K'_{11} & 0 \\ 0 & 0 & K'_{33} \end{bmatrix}, \quad (39)$$

where K'_{11} is as before and

$$K'_{33} = \begin{bmatrix} \frac{s_1}{Q_1} + \frac{T}{LQ_T} & \frac{\cos(\theta_1 - \theta_2)T}{LQ_T} & \dots & \frac{\cos(\theta_1 - \theta_k)T}{LQ_T} & \dots \\ \frac{\cos(\theta_1 - \theta_2)T}{LQ_T} & \frac{s_2}{Q_2} + \frac{T}{LQ_T} & & & \\ \vdots & & \ddots & & \\ \frac{\cos(\theta_1 - \theta_2)T}{LQ_T} & & & \frac{s_k}{Q_k} + \frac{T}{LQ_T} & \\ \vdots & & & & \ddots \end{bmatrix}$$

and

$$C = \begin{bmatrix} C_{11} & 0 & 0 \\ 0 & C_{11} & 0 \\ 0 & 0 & C_{22} \end{bmatrix}. \quad (40)$$

It is worth noting what the proportional damping assumption means in this particular context: if the body damping is proportional, then in a given mode the connection point at the bridge moves along a straight line (at the angle θ_k) as assumed here. If the body damping were not proportional, this would allow the possibility of a phase difference between the components of body motion, so that the contact point would travel around an ellipse.

3.4. The criterion for 'non-veering'

From the matrices derived in sections 3.1 and 3.3, it is simple to recover Gough's criterion for 'non-veering' mentioned earlier. At a frequency where modal overlap is low, it may be reasonable to approximate the behaviour when a string overtone falls close to a body resonance by keeping just the two generalised coordinates concerned. The system matrices then take the general form

$$M = \begin{bmatrix} m_1 & m_3 \\ m_3 & m_2 \end{bmatrix}, \quad K = \begin{bmatrix} k_1 & 0 \\ 0 & k_2 \end{bmatrix}, \quad C = \begin{bmatrix} c_1 & 0 \\ 0 & c_2 \end{bmatrix}, \quad (41)$$

where the individual symbols are defined by comparison with equations (17), (19) and (23). The complex natural frequencies are the roots ω of the equation

$$\det \{ -\omega^2 M + i\omega C + K \} = 0,$$

which reduces to

$$\begin{aligned} (\omega_1^2 + i\omega c_1/m_1 - \omega^2) \\ (\omega_2^2 + i\omega c_2/m_2 - \omega^2) &= \omega^4 \lambda^2, \end{aligned} \quad (42)$$

where

$$\omega_j^2 = k_j/m_j, \quad j = 1, 2,$$

and

$$\lambda^2 = m_3^2/(m_1 m_2).$$

This can be turned into a quadratic equation in ω^2 if the damping terms within the two bracketed expressions are approximated by

$$i\omega c_1/m_1 \approx i\omega_1^2/Q_1 \quad \text{and} \quad i\omega c_2/m_2 \approx i\omega_2^2/Q_2$$

in terms of the Q -factors Q_1 , Q_2 of the string and body modes respectively. At the tuned condition

$$\omega_1^2 = \omega_2^2,$$

the roots for $\Omega = \omega/\omega_1$ are then given by

$$\Omega^2 \approx \left[2 + i/Q_1 + i/Q_2 \pm \sqrt{4\lambda^2(1 + i/Q_1)(1 + i/Q_2) - (1/Q_1 - 1/Q_2)^2} \right] \cdot \left[2(1 - \lambda^2) \right]^{-1}. \quad (43)$$

The two roots are separated by an approximately real quantity if the expression inside the square root has a positive real part. This would mean that the two modes have similar Q factors but different frequencies, i.e. that veering has occurred. Conversely, if the expression inside the square root has a negative real part then the two modes have similar frequencies but different Q factors, as seen in Figure 1 for the non-veering case. Assuming small damping so that the two expressions $(1 + i/Q_j)$ inside the square root can be ignored, the condition for non-veering is thus approximately

$$4\lambda^2 < (1/Q_1 - 1/Q_2)^2. \quad (44)$$

The non-veering case illustrated in Figure 1 has $Q_1 = 3500$, $Q_2 = 100$, and $\lambda = 0.0035$, slightly below the threshold value of 0.0049 given by equation (44).

Substituting the actual values from equation (19), the condition becomes

$$\frac{8}{\pi^2 j^2 (1/3 + m_k/\rho L)} < \left(\frac{1}{Q_k} - \frac{1}{Q_{sj}} \right)^2, \quad (45)$$

or more interestingly

$$j^2 > \frac{8}{\pi^2 (1/3 + m_k/\rho L) (1/Q_k - 1/Q_{sj})^2}. \quad (46)$$

For a given string, only the lower modes are likely to couple strongly to body modes. Higher values of j are progressively more likely to satisfy this non-veering criterion.

To see what this means in practice requires numerical data. As will be described in section 4 and more fully in the companion paper [1], a plausible set of parameters has been determined for a particular guitar and its set of strings. Using these, condition (45) can be illustrated graphically. Each of the six strings is considered in turn, and for each string every note from the open string to the 12th fret is considered. For each of these notes, all string overtones below 2 kHz have been calculated, and for each of these the nearest body mode found, and the criterion (45) evaluated for this combination of string mode and body mode. Figure 2 shows the result: a symbol is plotted for every overtone at every fret on every string, showing the value of the right-hand side minus the left-hand side of this inequality. From the figure it is clear that “veering” behaviour (negative values) is only predicted for this guitar below about 300 Hz. Above that, the value of the plot-

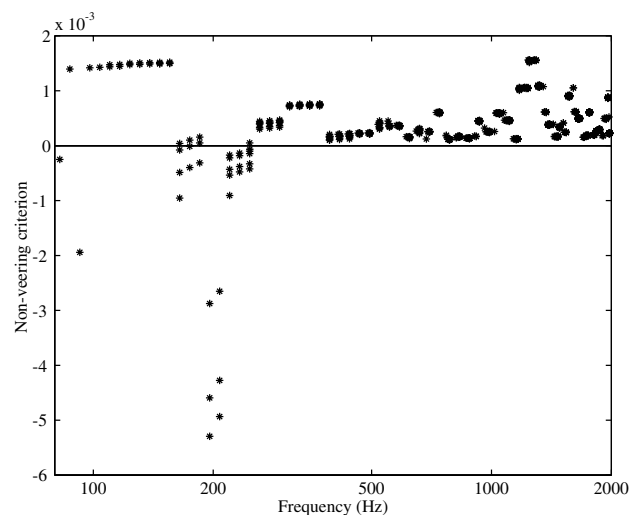


Figure 2. The “non-veering” criterion (45), for each overtone of every note on every string of a test guitar. Positive values indicate non-veering behaviour.

ted quantity is always positive so that “non-veering” is the rule. Synthesis using the undamped coupled modes and the Rayleigh estimate of damping is likely to give seriously misleading answers at all higher frequencies. Of course, the analysis described in this subsection will not apply strictly once the modal overlap becomes significant, but one might expect the qualitative conclusion to hold nevertheless. Detailed simulation comparisons will be shown in section 4.3.

A similar calculation can be carried out allowing for both polarisations of string motion: in other words, a pair of string modes coupled to one body mode. Equations (41) are replaced by 3×3 matrices extracted from equations (37), (38) and (40). However, it is not necessary to work through the details of this case to see what the answer will be. The string behaviour is rotationally symmetric: there is no significance to the particular two polarisation directions chosen, and any two orthogonal directions would give the same answer. However, the body mode behaviour is not rotationally symmetric: the chosen mode involves motion at the bridge at the appropriate angle θ_k , and in the perpendicular direction the body has no motion. The coupled string/body modes must respect the plane of symmetry associated with this body motion. The result is that string motion in the plane parallel to the body motion will couple to the body exactly as analysed above, while the perpendicular polarisation will be unaffected by body coupling.

This means that at frequencies where modal overlap in the body is low, so that this approximation should hold, one string polarisation is uncoupled to the body motion and therefore unable to radiate sound. The player will in general excite a mixture of both polarisations, and they will vibrate with two different decay factors, but the radiated sound will show little trace of the “double decay” which occurs in other systems with similar behaviour, such as coupled piano strings [33]. The slow-decaying mode can only radiate via distant modes which have a differ-

ent angle θ_k . (This simple result would change if non-proportional damping of the body mode was allowed, so that the body motion was no longer along a single line.) At higher frequencies where modal overlap in the body becomes significant the behaviour may be different: a given string overtone will couple significantly to more than one body mode, with different values of θ_k , and it is likely that both polarisations would couple to body motion and thus be able to radiate sound to some extent. To assess what really happens at these higher frequencies is one of the major reasons for carrying out full syntheses using both string polarisations. Results will be shown in section 4.5.

3.5. Body coupling via the fingerboard

So far, it has been assumed that the string couples to the body only at the bridge. However, in reality there will obviously be some coupling through the nut or fret. Published measurements of the admittance of a typical guitar at the frets [34, 35] suggest that this would make only a small difference to the predictions, so it will not be taken into account in the remainder of this paper. However, it would be straightforward to extend the methods developed here to allow for a non-rigid nut or fret. For the modal methods, additional constraint modes would be included which would be the mirror image of those used so far: moving at the fret but fixed at the bridge. To extend the frequency-domain methods requires a little more care, since the coupling would no longer be at a single point. However, the matrix version of the coupling formula (9) can be extended to multiple-point coupling, by assembling matrices which contain as many dimensions as there are degrees of freedom constrained by the coupling: they will be 2×2 matrices if one string polarisation is allowed, and 4×4 if two are allowed. Note that these matrices would involve not only the admittances at the bridge and fret, but also the transfer admittances between bridge and fret.

The most likely context in which string/body coupling through the frets might be significant is for the higher frets which lie over the soundboard rather than on the neck. It is a common complaint of guitar players that some notes in these positions “fall flat”, presumably implying a decay rate more rapid than is desirable. Guitar makers often include additional bracing under this area of the soundboard to reduce the problem. Another context in which coupling at the fret might be important would be in analysing the behaviour of solid-body electric guitars. Although the body vibration does not directly produce the sound, the decay times of the strings are still of great concern to players, and these decay times are governed by mechanical rather than electrical effects. One would guess that in this case the energy loss through the frets might be greater than that through the bridge.

4. Comparisons between methods

4.1. The test case

The modal and frequency-domain synthesis methods described in section 2 can now be implemented and tested.

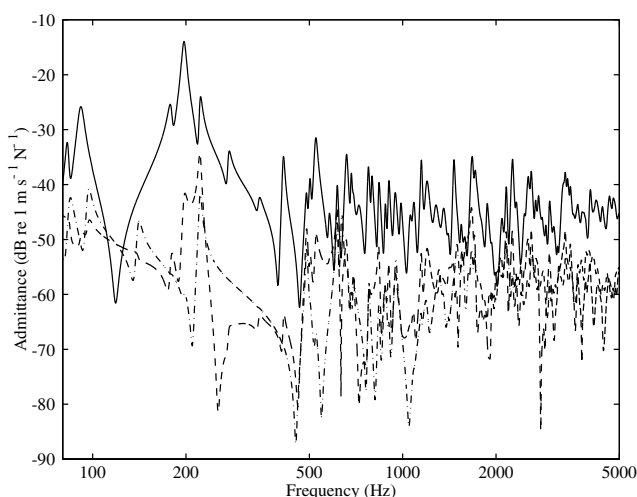


Figure 3. Calibrated admittances Y_{11} (solid line), Y_{12} (dashed line) and Y_{22} (dash-dot line) determined from a test guitar by measurement followed by modal fitting, as described in the text and more fully in [1].

For comparisons between methods in this section, a standardised test case will be used. This relates to the lowest note of a normally-tuned guitar, the open E string (82.41 Hz). The string length is 650 mm, and the string properties correspond to a D’Addario “Pro Arte composite, hard tension” string: tension 71.6 N, mass per unit length 0.0062 kg/m, string Q factor assumed to be 3500 for all modes, and bending stiffness $5.7 \cdot 10^{-5} \text{ Nm}^2$. Modal-based methods allow for 65 string modes, giving a maximum frequency of 5211 Hz (including the effect of bending stiffness). The value for bending stiffness comes from measurements reported in the companion paper [1]. The constant- Q damping model is not realistic, but the numerical value used here is of the correct order of magnitude for the mid-frequency overtones of the string.

The determination of the body vibration model is also explained in the companion paper [1]. It uses 240 modes, up to a maximum frequency of 5190 Hz. Up to 1500 Hz the modal parameters of mass, frequency, damping and angle were explicitly fitted to the measured admittance matrix of a test guitar. The higher modes were determined by a “statistical fit” to the measurements, which uses a random number generator to give frequencies with the correct density and spacing statistics, as well as damping factors, modal masses and angles with approximately the correct statistical distribution. The resulting admittances Y_{11} , Y_{12} and Y_{22} are plotted in Figure 3.

For each method tested, a pluck at a point 20 mm from the bridge has been synthesised. For methods involving both polarisations of string motion, a plucking angle of 45° to the normal to the soundboard is assumed. The output variable is the acceleration of the body at the bridge, in the normal direction. This is a convenient quantity for comparison with experiments, to be discussed in the companion paper. It is also the simplest quantity which approximately mirrors the spectral characteristics of the radi-

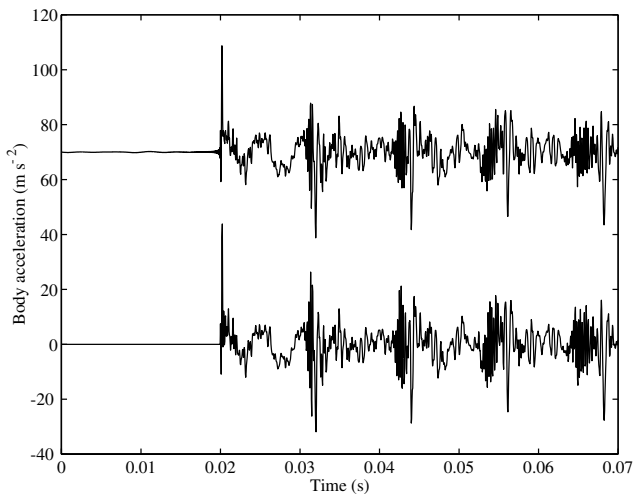


Figure 4. Comparison of the first few cycles of synthesised plucks using the frequency domain method (upper curve) and the first-order modal method (lower curve). Body acceleration in response to a pluck amplitude of 1 N is plotted. The upper curve is offset for clarity.

ated sound (but keep in mind that modal radiation efficiencies are not included here). Plucks were synthesised with a sampling rate of 22050 Hz, high enough that the Nyquist frequency is well above the highest frequency included in the model. For efficiency of the frequency-domain methods, the length of the synthesised pluck was chosen to have 2^{17} samples to expedite FFT calculation. This results in a synthesis time of 5.94 s, a time chosen to be long enough to minimise “leakage” problems in the methods which use an inverse FFT to obtain the transient response.

4.2. Accuracy and speed

All the synthesis methods were coded in Matlab, using vectorised constructions wherever possible to maximise speed. The first question to ask is whether all the methods will run at all given the complexity of the problem. The answer to this is affirmative: in particular, Matlab’s eigenvalue/eigenvector routine was able to cope with both styles of modal synthesis. For the first-order method with both string polarisations, the matrix A has dimension 700 and is not sparse, so it was not obvious *a priori* that the calculation would be accurate. However, no difficulty was encountered.

To check whether the computed answers are reliable, it is useful to compare results by the first-order modal method (based on equation 25) with corresponding results by the frequency domain approach (equation 8) using the damped-string results (29) and (31). These two methods use entirely independent approaches and coding, but embody similar approximations. Figures 4 and 5 show that excellent agreement can be obtained between these two methods, when applied to the most challenging case with both string polarisations. Figure 4 shows a time-domain comparison of the first few cycles following the pluck. The frequency-domain method shows motion at very low am-

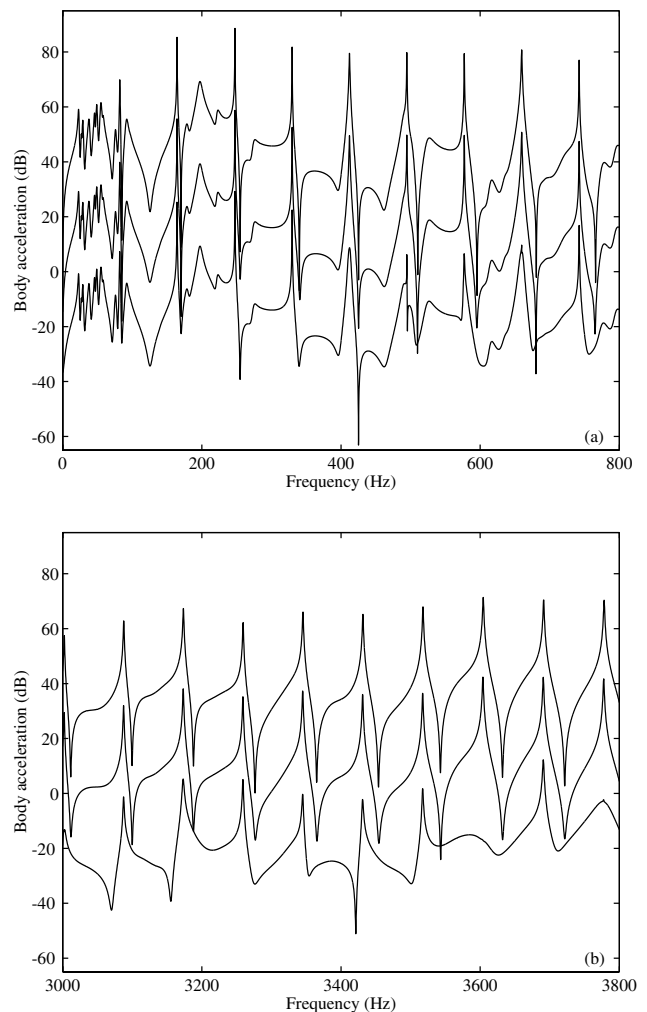


Figure 5. Comparison of the Fourier spectrum of synthesised plucks using the frequency domain method (upper curve), the first-order modal method (middle curve) and undamped modes plus Rayleigh’s principle (lower curve). The curves are offset for clarity: the upper curve shows the true values. Plots (a) and (b) show the same spectra over different frequency ranges.

plitude before the pluck, because of the finite length and resolution of the inverse FFT, but this seems acceptably small. The top two curves of Figure 5a show a frequency-domain comparison of the two plucks at low frequencies. Again, excellent agreement between the two methods is shown: the only visible deviations occur near the antiresonances. This time, as one would expect, the frequency-domain approach gives the more accurate answers while the first-order modal approach shows minor errors due to the finite FFT used to generate the plot. This level of agreement extends over the entire frequency range of the synthesis: Figure 5b shows a typical comparison at higher frequencies. The conclusion is that both methods give an accurate synthesis for the test case, whether one or two string polarisations is required.

Timings for a selection of synthesis methods are given in Table I. The absolute times are of little significance because they depend on the machine and the detailed coding,

Table I. Timing of selected synthesis methods for a 6-second plucked note including string and body modes up to 5 kHz (see text for details). The timings of frequency domain methods assume pre-calculation of the body admittance(s), which are read from a saved file. A quirk of the Matlab code used for these tests is that the apparently simple case of the undamped modal method with only one string polarisation gave a persistent error from the eigenvalue routine, so that case is not included. Pol.: Polarisation.

Method	Pol.	String modes	Time [s]
Undamped modal/Rayleigh	2	damped	137
Modal first order	1	damped	215
Modal first order	2	damped	325
Frequency domain	1	undamped	1.6
Frequency domain	2	undamped	1.9
Frequency domain	1	damped	23
Frequency domain	2	damped	23
Time domain	1	damped	798

but the relative speeds of different methods are of interest. Two things stand out from this table. First, the modal methods are significantly slower than the frequency-domain methods. Indeed, the frequency domain approach is impressively fast: provided the body admittance is calculated first and saved, since it is the same for every note on the chosen string, the slowest frequency domain synthesis method running in Matlab took 23 s for this 6 s note, only a factor of four slower than real-time performance. The second conspicuous feature of Table I is the last entry: this shows the time for the digital waveguide simulation of the standard case, with one string polarisation only. Even if the method had given the correct answer it would have been hopelessly slow, at least in this style of implementation.

4.3. Modal methods and “non-veering”

Next it is of interest to compare the performance of the two types of modal synthesis. The earlier discussion of “non-veering” behaviour, and the prediction of Figure 2, suggest that the two methods might give similar results at low frequencies, where the string/body coupling is relatively strong, but that the method based on undamped modes may be seriously misleading at higher frequencies. The synthesis results bear out this expectation. Figure 5 shows frequency-domain comparisons of the two methods, for the case with two string polarisations: the top two curves, already discussed, show the “correct” result, and the lower curve shows the results based on undamped modes and Rayleigh’s principle. Figure 5a shows the low frequency range, and all three curves are indeed very close together throughout this range (although there are some disparities in peak height, hard to see in the plot). However, Figure 5b shows a typical sample of the behaviour at higher frequency, and now the methods give quite different results. The first-order method shows “string modes” with very little visible trace of body effects, whereas the method based on undamped modes shows strong influence from the body. For any synthesis extending beyond

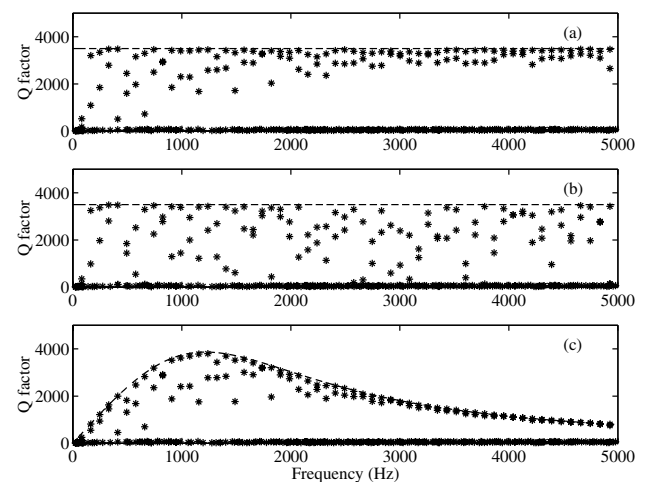


Figure 6. Computed Q -factors from three different synthesis methods: (a) the first-order modal method, assuming constant string damping; (b) the undamped modal method plus Rayleigh’s principle, assuming constant string damping; (c) the first-order modal method using frequency-dependent string damping as determined from measurements [1]. In each case the dashed line shows the string damping as a function of frequency. The low- Q modes near the horizontal axis are “body modes”.

a few hundred Hertz the undamped-mode method would give answers which are sufficiently wrong that the difference would almost certainly be audible (although comparative listening tests have yet to be conducted).

An important consequence of “non-veering” behaviour is illustrated in Figure 6. It was shown in Figure 1b that veering behaviour leads to a strong increase of damping of the “string” modes near a body resonance, whereas “non-veering” implies a much smaller influence on damping from body coupling. Figure 6a shows the Q factors of all modes up to 5 kHz as computed by the first-order method, while Figure 6b shows the corresponding results for the Rayleigh method. Except at the lowest frequencies, Figure 6a shows a very clear split between “body modes” with low Q and “string modes” with high Q . Figure 6b shows a much wider scatter of Q -factors, as expected. Both these plots correspond to the test case discussed above, in which the intrinsic damping of the string was assumed to be independent of frequency. Figure 6c shows the first-order results when a more accurate model of string damping is used, as will be explained in detail in the companion paper [1]. There is still a clear distinction between body modes and string modes, but at the higher frequencies the disparity of damping is much lower since the effect of damping associated with string bending stiffness makes itself felt.

Another view of the damping of “string modes” by body coupling is given by Figure 7. By synthesising plucked notes on the lowest string of the instrument at a variety of pitches and then combining the decay data, a relatively smooth curve can be plotted of decay rate against frequency. Specifically, frequency-domain syntheses have been carried out for each note of the lowest string from the open string to the 12th fret, plucked normal to the sound-

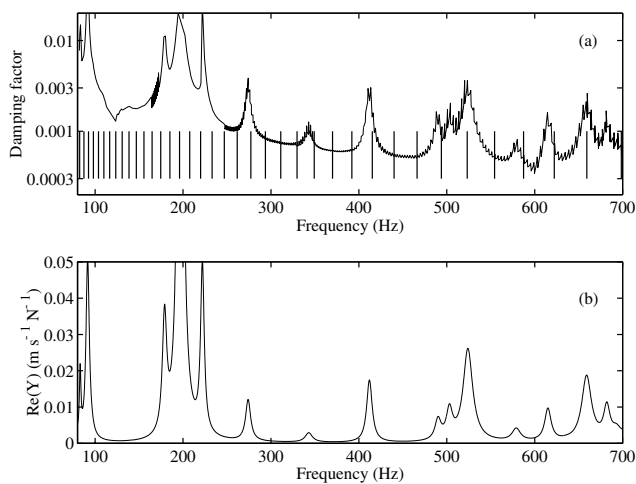


Figure 7. Damping factor of “string modes” as a function of frequency (a) compared to $\text{Re}\{Y_{11}\}$ (b). Pluck transients were synthesised using the same model as for Figure 6c, on the lowest string, plucking normal to the soundboard, at every fret up to the 12th and with the tension varied in ten steps so that the fundamental pitch varied in 10 cent increments. Each transient was analysed by a sonogram-fitting technique described in [1] to obtain damping factors. Vertical lines in (a) indicate the fundamental frequencies of equal-tempered notes in the usual pitch standard.

board, and the series was repeated for ten increments of the string tension so that the gaps between semitones were covered in 10 cent steps. For each transient, the decay rates were computed using a sonogram technique described in detail in the companion paper [1]. Arranging all the results into frequency order and then plotting over the range up to 1 kHz, where from Figure 6 it is expected that body coupling will be significant, gives the result shown in Figure 7a. For comparison, Figure 7b shows $\text{Re}\{Y_{11}\}$ on the same frequency scale. This quantity would be expected to account for the dominant energy loss from string to body, and indeed the similarity of the two curves is striking.

Figure 7a contains information of interest to guitar makers and players. For the particular guitar on which this synthesis model is based, the high peak near 520 Hz falls close to an equal-tempered note in standard tuning, and players often complain about this note “falling flat”. It can be seen in the figure that the peak is quite narrow, and at this frequency a semitone corresponds to a frequency jump of about 31 Hz. (The fundamental frequencies of equal-tempered notes for normal tuning are shown as vertical lines in Figure 7a.) A half-semitone shift of tuning would be enough to reduce the peak damping factor by a factor of approximately four. This shows why guitars of apparently similar construction may differ widely in the perception of notes like this “falling flat”: they all possess essentially the same resonant modes at these low frequencies, but a small shift in frequency of this body resonance to place it between two notes rather falling exactly on a note could account for the difference in perceived effect.

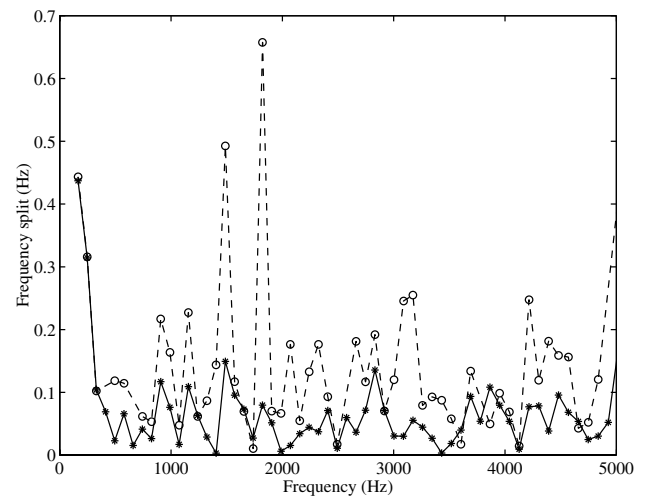


Figure 8. Frequency split in Hz between the pairs of “string modes” computed by the first-order modal method (solid line); and the undamped modal method plus Rayleigh’s principle (dashed line).

A final aspect of non-veering is illustrated in Figure 8. As expected, the “string modes” appear in pairs representing the two polarisations of motion. The frequency split between each pair is of interest, both as a measure of body coupling and as an aspect of string behaviour which may have directly audible consequences. The splits are plotted, for both modal methods of calculation. It is clear that the frequencies computed via undamped modes are split somewhat more widely, as the veering argument suggests. The splits according to the first-order method are only about 0.1 Hz over the entire frequency range. This would suggest that, even if both polarisations of string motion were audible, the beat periods would be of the order of 10 s or longer, and since the higher overtones of string motion do not last as long as 10 s one might predict very little audible effect.

4.4. Use of the undamped string model

It is of some interest to see the results of synthesis using the frequency domain approach without allowing for the string’s intrinsic damping. If the results (26) and (27) are used in place of (31) and (29) respectively, a result is obtained which is illustrated in Figure 9. This shows the first 0.5 s of the transient compared to the corresponding result when the string damping is included. It is immediately clear that the two results are very different. There are two reasons for this difference. One concerns the string damping directly: it has already been seen that high-frequency string modes couple very weakly to the body and thus retain low damping, so if the string has no intrinsic damping at all this can lead to very slow decay being predicted. The second reason for difference between these methods is that the damped-string formulae take the form of modal sums, which can be truncated at the assumed number (65) of string modes. However, the closed-form results (26) and (27) do not lend themselves so easily to this, and the

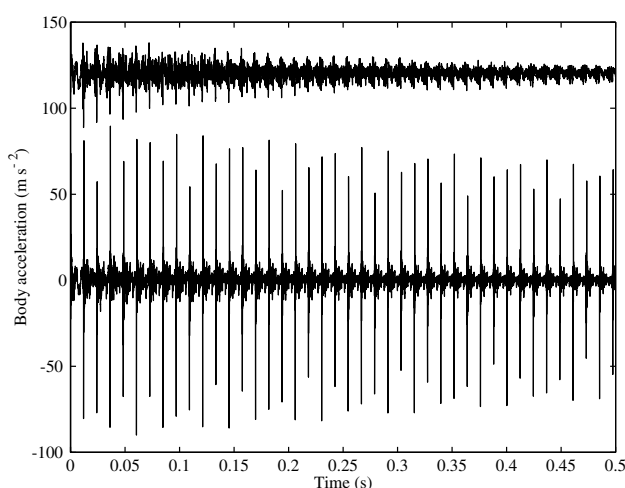


Figure 9. Comparison of synthesised plucks using the frequency domain method with the damped string model (upper curve) and the undamped string model (lower curve). Body acceleration in response to a pluck amplitude of 1 N is plotted. The upper curve is offset for clarity.

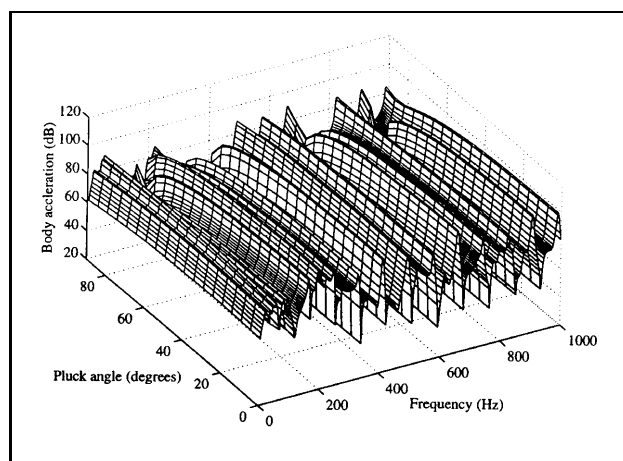


Figure 10. Frequency spectrum of body acceleration following a pluck, as a function of plucking angle from the normal to the guitar soundboard.

synthesis includes string behaviour up to the Nyquist frequency. Of course, if this were the only problem a filter of some kind could be included, but since the damped-string formulae work so well there is no obvious incentive to explore this possibility.

4.5. The response to varying pluck angle

It is now clear that the preferred synthesis method for this kind of “laboratory” use is the frequency domain approach using damped string behaviour – it is both accurate and fast. (The method would be less suitable for real-time musical synthesis, even with a faster implementation, because the FFT method has an intrinsic latency which would be unacceptable.) This method can now be used to show the effect on the body motion, and hence ultimately on the sound, of the orientation of the initial pluck. Obviously, this is a question which can only be posed in the context of

a model including both polarisations of string motion. At least roughly, a rotation of the plane of the initial pluck will correlate with differences of playing technique: for example, between *apoyando* and *tirando* finger strokes (see for example [36]). Figure 10 shows how the spectrum of body acceleration in the normal direction varies with pluck angle, from zero (normal to the soundboard) to 90° (parallel to the soundboard). The plot shows that the changes are rather small until the angle reaches about 70° , but then there are rapid and significant changes as the angle moves towards 90° . The effects are different for different frequencies (because of the influence of the modal angles θ_k), but many of the strong frequency peaks show a drop by 20–30 dB in this range. At a few frequencies, a rise in amplitude can be seen over the same range of angles. This plot confirms something which is well known to guitarists, that the exact way that a pluck is executed can have a very significant influence on the sound.

5. Conclusions

A variety of different approaches have been described to the problem of synthesising the pluck response of a guitar. All methods start from the same information: string properties and input admittance at the bridge of the guitar. Synthesis can be carried out in the frequency domain, the time domain, or via modal superposition. Within these broad categories there are further options. A range of these methods has been implemented, and their performance on a particular test case has been compared. The test case was based on the lowest note of the guitar, and aimed to synthesise the response up to approximately 5 kHz. This is a non-trivial task, for example involving some 350 degrees of freedom in the modal methods.

Some synthesis methods were found to give unsatisfactory results: time domain synthesis via the “digital waveguide” approach, modal synthesis based on first solving for the undamped system modes, and any method which does not allow for the inherent damping of the string (although this is very low). Two methods remain, which both gave predictions in accurate agreement with one another: modal synthesis using the first-order method, and frequency-domain synthesis incorporating the effect of string damping. Of the two, frequency domain synthesis proved to be faster by a significant factor, and this is recommended as the method of choice.

Many of the problems besetting the unsuccessful methods revolve around the treatment of vibration damping. In particular, post-processing the undamped modes, a method which works well in many vibration problems, can give very inaccurate answers for the guitar problem, mainly because the system as a whole exhibits strongly non-proportional damping: the inherent damping of the string is much lower than that of the body. Modelling of this phenomenon shows that at frequencies above a few hundred Hertz, the coupled string/guitar system does not show “veering” behaviour, and this allows lightly-damped “string modes” to occur at high frequencies, even though

the body exhibits significant modal overlap so that there is always a body mode close enough that coupling would be expected.

It must be emphasised, though, that the tests shown in this paper have only compared synthesis methods with one another. The “winning” methods give consistent answers by very different routes, and to that extent seem to be reliable. However, to know whether these answers are in fact the correct ones requires comparison with experiment. That task is taken up in a companion paper [1].

Acknowledgement

The author thanks Bernard Richardson and Robin Langley for helpful discussions, and Martin Woodhouse for assistance and for providing the test guitar.

References

- [1] J. Woodhouse: Plucked guitar transients: comparison of measurements and synthesis. *Acustica/acta acustica* (Companion to this).
- [2] L. Cremer: *The physics of the violin*. MIT Press, Cambridge MA, 1985.
- [3] C. Valette: The mechanics of vibrating strings. – In: *Mechanics of Musical Instruments*. A. Hirshberg, J. Kergomard, G. Weinreich (eds.). Springer-Verlag, Vienna, 1995.
- [4] N. C. Pickering: *The bowed string*. Ameron, Mattituck, New York, 1992.
- [5] N. H. Fletcher, T. D. Rossing: *The physics of musical instruments*. Springer-Verlag, New York, 1990.
- [6] C. E. Gough: The theory of string resonances on musical instruments. *Acustica* **49** (1981) 124–141.
- [7] J. C. Schelleng: The violin as a circuit. *J. Acoust. Soc. Amer.* **35** (1963) 326–338.
- [8] G. Derveaux, A. Chaigne, P. Joly, E. Bécache: Time-domain simulation of a guitar: model and method. *J. Acoust. Soc. Amer.* **114** (2003) 3368–3383.
- [9] R. R. Craig: *Structural dynamics*. Wiley, N.Y., 1981.
- [10] M. Laurson, C. Erkut, V. Välimäki, M. Kuuskankare: Methods for modeling realistic playing in acoustic guitar synthesis. *Computer Music J.* **25** (2001) 38–49.
- [11] G. Weinreich: Vibration and radiation of structures. – In: *Mechanics of Musical Instruments*. A. Hirshberg, J. Kergomard, G. Weinreich (eds.). Springer-Verlag, Vienna, 1995.
- [12] E. Skudrzyk: *Simple and complex vibratory systems*. Pennsylvania State University Press, Pennsylvania, 1968.
- [13] O. Christensen, B. B. Vistisen: Simple model for low-frequency guitar function. *J. Acoust. Soc. Amer.* **68** (1980) 758–766.
- [14] A. H. Benade: *Fundamentals of musical acoustics*. Oxford University Press, London, 1976.
- [15] M. E. McIntyre, J. Woodhouse: The influence of geometry on linear damping. *Acustica* **39** (1978) 209–224.
- [16] M. E. McIntyre, J. Woodhouse: On measuring the elastic and damping constants of orthotropic sheet materials. *Acta Metallurgica* **36** (1988) 1397–1416.
- [17] N. C. Perkins, C. D. Mote: Comments on curve veering in eigenvalue problems. *J. Sound Vib.* **106** (1986) 451–463.
- [18] Lord Rayleigh: *Theory of sound*, Vol. 1. Dover Publications, New York, 1945.
- [19] J. Woodhouse: Linear damping models for structural vibration. *J. Sound Vib.* **215** (1998) 547–569.
- [20] S. Adhikari, J. Woodhouse: Quantification of non-viscous damping in discrete linear systems. *J. Sound. Vib.* **260** (2003) 499–518.
- [21] T. K. Caughey: Classical normal modes in damped linear dynamic systems. *J. Applied Mech.* **27** (1960) 269–271.
- [22] D. E. Newland: *Mechanical vibration analysis and computation*. Longman Scientific and Technical, Harlow, 1989.
- [23] B. E. Richardson: Simple models as a basis for guitar design. *J. Catgut Acoust. Soc. Series II, 4* **5** (2002) 30–36.
- [24] G. Bissinger: Modal analysis of a violin octet. *J. Acoust. Soc. Amer.* **113** (2003) 2105–2113.
- [25] A. Chaigne: On the use of finite differences for musical synthesis: application to plucked stringed instruments. *Journal d’Acoustique* **5** (1992) 181–211.
- [26] M. E. McIntyre, R. T. Schumacher, J. Woodhouse: On the oscillations of musical instruments. *J. Acoust. Soc. Amer.* **74** (1983) 1325–1345.
- [27] J. Woodhouse: On the playability of violins. Part I: reflection functions. *Acustica* **78** (1993) 125–136.
- [28] J. Woodhouse, R. T. Schumacher, S. Garoff: Reconstruction of bowing point friction force in a bowed string. *J. Acoust. Soc. Amer.* **108** (2000) 357–368.
- [29] J. Woodhouse, A. R. Loach: The torsional behaviour of cello strings. *Acustica – Acta Acustica* **85** (1999) 734–740.
- [30] J. Woodhouse: On the playability of violins: Part 2, Minimum bow force and transients. *Acustica* **78** (1993) 137–153.
- [31] J. G. Proakis, D. G. Manolakis: *Digital signal processing*. Prentice-Hall, New Jersey, 1996.
- [32] R. W. Clough, J. Penzien: *Dynamics of structures*. McGraw-Hill, New York, 2nd edition 1993: see section 14.7.
- [33] G. Weinreich: Coupled piano strings. *J. Acoust. Soc. Amer.* **62** (1977) 1474–1484.
- [34] R. R. Boullosa: Admittance at the frets of a classical guitar. *J. Catgut Acoust. Soc. Series II, 4* **4** (2001) 33–36.
- [35] R. R. Boullosa: A note on the sound radiation from the classical guitar: influence of energy input via the string termination at the fret. *Acustica – Acta Acustica* **89** (2003) 718–721.
- [36] G. Wade: *The triumph of the Segovia technique. The classical guitar book*. Backbeat Books, San Francisco, 2002.